Biomedicine & Pharmacotherapy 188 (2025) 118193

Contents lists available at ScienceDirect

Biomedicine & Pharmacotherapy

journal homepage: www.elsevier.com/locate/biopha

Formation of a triple complex of viral capsid protein 1 and two capsid-binding inhibitors explains synergistic interactions observed in combination studies with rhinoviruses

Martina Richter [a,1], Maria Khrenova [b,c,1], Olga Riabova [b], Vadim Makarov [b], Michaela Schmidtke [a,*]

[a] Jena University Hospital, Institute of Medical Microbiology, Section Experimental Virology, Hans-Knoell-Str. 2, Jena 07743, Germany
[b] Federal Research Centre "Fundamentals of Biotechnology" of the Russian Academy of Sciences (Research Centre of Biotechnology RAS), 33-2 Leninsky Prospect, Moscow 119071, Russia
[c] cDepartment of Chemistry, Lomonosov Moscow State University, 1/3 Leninskie Gory, Moscow 119991, Russia

ARTICLE INFO

Keywords:
Common cold
Antiviral combination
Pleconaril
OBR-5–340
Synergism
Molecular mechanism

ABSTRACT

Capsid-binding inhibitors, such as pleconaril and OBR-5-340, which prevent the attachment and/or uncoating of most rhinovirus (RV) types, were considered promising candidates for effective anti-RV drug development. Both inhibitors target viral protein 1 (VP1), but their efficacy, spectrum of anti-RV activity, and binding mechanism are different. We hypothesized that combinations of pleconaril and OBR-5–340 might be a promising approach to improve treatment strategies for RV infections. To validate our hypothesis, we analyzed the anti-RV effects of a 6 × 6 concentration matrix compared to monotherapy *in vitro*. Antiviral studies included multiple RV types, some of which are sensitive or insensitive to pleconaril and OBR-5-340, to consider the diversity of VP1. Synergy analysis was performed with Loewe additivity, Bliss independence, highest single agent, and zero interaction potency models. The results indicate a significant synergistic effect at certain concentrations. Molecular dynamic simulations investigated the molecular basis of the observed synergy. Intriguingly, VP1, pleconaril and OBR-5–340 can bind simultaneously to form a triple complex with additional stabilizing hydrophobic interactions and hydrogen bonds. Consequently, pleconaril-OBR-5–340 combination surpassed the efficacy of monotherapy and inhibited a broader RV spectrum compared to monotherapy. In conclusion, this study contributes to the development of broader-spectrum anti-RV treatments and provides insights into the mechanism behind. This strategy could also be important for treatment of diseases caused by other enteroviruses. The identified strong synergism warrants further preclinical studies for example with, *ex vivo* or human viral challenge models to translate this synergy into oral or inhaled/topical use for rhinovirus treatment.

1. Introduction

Rhinoviruses (RV types) belong to the genus *ENTEROVIRUS* of the family *Picornaviridae.* RV types are classified into the species *Rhinovirus A*, *B*, and *C* (*RV-A*, *RV-B*, and *RV-C*) [36]. Their simple structure includes a positive-sense, single-stranded RNA which is packaged in an icosahedral capsid. The capsid is composed of each sixty copies of four viral proteins (VP1–4). There are about 160 RV types. The majority of RV types belong to *RV-A* and *RV-B* and possess a highly conserved hydrophobic pocket in VP1 [7,21].

The high number of RV types represents a great challenge in the development of effective direct-acting antiviral drugs. The drugs need to act preferably against the majority or even all RV types (broad-spectrum activity) [31,39]. Broad-spectrum drugs would have the potential to effectively treat RV-caused diseases including common cold, bronchitis or pneumonia [7,11,38]. They could also prevent exacerbations of asthma, chronic obstructive pulmonary disease, and secondary infections caused by bacteria [15,16].

Abbreviations: Bliss, Bliss independence; CPE, cytopathic effect; Hpi, hours post infection; HAS, highest single agent; EC50, inhibitory concentration 50 %; Loewe, Loewe additivity; MSAS, most synergistic area score; RV, rhinovirus; VP1-4, virus capsid proteins 1–4; ZIP, Zero interaction potency.

* Correspondence to: Jena University Hospital, Department Medical Microbiology, Section Experimental Virology, Hans-Knoell-Str. 2, Jena 07743, Germany.
E-mail address: michaela.schmidtke@med.uni-jena.de (M. Schmidtke).

[1] Shared first co-authorship: Martina Richter and Maria Khrenova contributed equally to the manuscript.

https://doi.org/10.1016/j.biopha.2025.118193
Received 27 February 2025; Received in revised form 12 May 2025; Accepted 21 May 2025
Available online 26 May 2025

The discovery of the capsid-binding inhibitor (capsid binder) pleconaril proved the capability to identify and develop anti-RV drugs with broad-spectrum activity. Pleconaril strongly inhibits the majority of *RV-A* and *RV-B* by fitting into the highly conserved hydrophobic pocket in VP1 and blocking viral uncoating [21,46]. However, pleconaril has not been approved for the common cold treatment due to its drug's safety profile [33]. It induces cytochrome P-450 3 A enzymes (CYP3A4), which metabolize a variety of drugs [10,23,24]. In addition, ~10 % of known RV A and B types [21] and clinical RV isolates [18,26] have been shown to be pleconaril-insensitive. These limitations have necessitated the development of next-generation capsid binders with improved efficacy and safety profiles. In the result novel broad-spectrum capsid binder with high level of bioavailability were discovered that strongly inhibit pleconaril-insensitive RV types and/or do not induce or inhibit CYP3A4 [3,6]. The pyrazolopyrimidine OBR-5–340, which binds close to the entrance of the hydrophobic pocket in VP1 of RV types, is one of these capsid binders [25,29,43]. Hence, pleconaril and OBR-5–340 belong to the most deeply and extensively studied broad-spectrum anti-RV agents with a capsid-binding mechanism of action. Intriguingly, they act at different sites of the same target, VP1.

There are no anti-RV therapies today. As has been shown for human immunodeficiency virus (HIV) and hepatitis C virus today [35] effective combinations of antiviral drugs represents a promising strategy to fill this gap. Antiviral drug combinations typically target multiple viral proteins. In addition, some combinations of drugs binding to different sites of a viral protein exist. Combinations of antiviral agents were also investigated to identify treatment options for infections with enteroviruses including RV types [12,14,40]. No previous studies have explored the combined effect of broad-spectrum capsid binders with different anti-RV activity spectrum and binding site at the same target as found for pleconaril and OBR-5–340.

Today several reference models exist for analyzing drug interactions with respect to synergistic and antagonistic effects. Loewe additivity (Loewe), Bliss independence (Bliss), highest single agent (HSA), and zero interaction potency (ZIP) models are commonly used. They provide sufficient evidence of combination effects in preclinical studies [8,13,42,44,47].

We hypothesized that the combination of two structurally distinct capsid-binding inhibitors (pleconaril and OBR-5–340) would form a stable triple complex with VP1, leading to enhanced antiviral efficacy. Based on knowledge of RV biology and activity of capsid-binding RV inhibitors [21,25,43,46], as discussed above, we included multiple RV types with known sensitivity or insensitivity to pleconaril and OBR-5–340 in antiviral combination studies in Hela cells. We used HSA, Loewe, Bliss, and ZIP reference models to prove the enhanced antiviral efficacy of pleconaril-OBR-5–340 combinations compared to monotherapy in vitro. We performed molecular dynamics simulation with pleconaril, OBR-5–340, and VP1 to see if a ternary complex may underlie the observed synergy. Thus, extensive experimental and theoretical studies were conducted to illustrate the potential synergism between the two capsid-binding inhibitors and to explain the observed findings.

2. Materials and methods

2.1. Compounds, cells, and viruses

The study was performed with the two broad-spectrum capsid binders OBR-5–340 and pleconaril. Their structure (Fig. 1), synthesis, cytotoxicity, spectrum of anti-RV activity, molecular binding mechanism, and pharmacokinetics (*in vivo* and/or human) were well known [1,2,19,20,25,43,46]. OBR-5–340 and pleconaril were chosen together because they strongly differ in their activity against multiple RV types and target different binding sites in VP1. Stock solutions (10 mM) of OBR-5–340 and pleconaril were prepared in dimethyl sulfoxide and methanol, respectively.

HeLa Ohio cells (HeLa; human cervix carcinoma; FlowLabs, USA) were grown in Eagle's minimal essential medium (EMEM; Lonza, Basel, Schweiz) supplemented with 2 mM L-Glutamin (Lonza, Basel, Schweiz), and 10 % neonatal calf serum (PAA, Cölbe, Germany). The test medium contained only 2 % of serum.

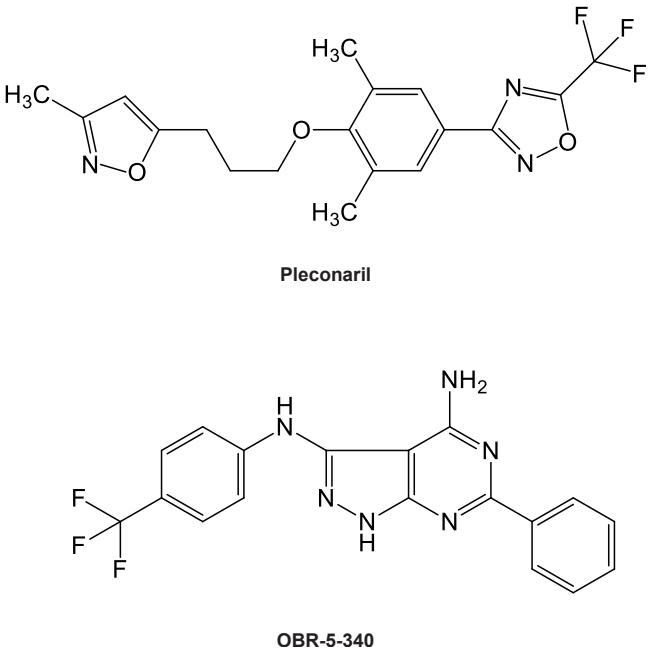

Fig. 1. Structure of pleconaril and OBR-5–340.

Our screening platform included three sets of each three RV types with distinct pleconaril and OBR-5–340 sensitivity [25]. The three sets consider the three major sensitivity pattern detected for both inhibitors [30]:

(i) RV-B5, RV-B48, and RV-B69: pleconaril-insensitive (no activity at non-cytotoxic concentrations), but highly OBR-5–340-sensitive (50 % inhibitory concentration (IC_{50}) < 1 μM) used in analogy to the published half-maximal effective concentration of pleconaril [26] because there are no clinical data,
(ii) RV-A8, RV-B17, and RV-B52: pleconaril- and OBR-5–340-sensitive RV types (IC_{50} > 1 μM to both compounds), and
(iii) RV-A2, RV-B3, and RV-B70: highly pleconaril-sensitive (IC_{50} < 1 μM), OBR-5–340-sensitive (IC_{50} > 1 μM).

Working passages of RV-A2, RV-B3 (Medical University of Vienna, Vienna, Austria), RV-B5, RV-B17, RV-B48, RV-B52, and RV-B69 (National Collection of Pathogenic Viruses, Salisbury, Great Britain), RV-A8 (Avir Green Hills Biotechnology AG, Vienna, Austria), RV-B70 (Rega Institute for Medical Research, University of Leuven, Leuven, Belgium) were prepared and titered in HeLa cells before [25,30].

2.2. Antiviral combination studies

The antiviral effect of (i) pleconaril monotherapy, (ii) OBR-5–340 monotherapy, and (iii) of pleconaril-OBR-5–340 combinations was evaluated using cytopathic effect (CPE) inhibition assay in one-day-old semi confluent HeLa cells grown in a 96-well tissue culture plate (Biochrom AG, Berlin) as described previously [25,32].

Earlier determined 50 % inhibitory concentration (IC_{50}) values of both inhibitors [25] provided the base for choosing the appropriate dosage ranges (Supplementary Table 1). The concentrations cover the expected range of activity upon and below the IC_{50} values for the tested RV types [42]. The selected concentrations of the individual inhibitors did not exert cytotoxicity in HeLa cell monolayers upon 72 h of treatment as published previously [25]. Because combinations could still

interact differently, combination-specific cytotoxicity tests are planned but not yet performed.

Briefly, after removal of the cell culture medium we added 50 µl of double-concentrated (i) pleconaril or (ii) OBR-5–340 solutions (monotherapy: 6 concentrations as used in combination; dilution factor 2) and 50 µl of a virus suspension, or (iii) 25 µl of each compound solution (fourfold-concentrated; 6 × 6 concentration matrix) and 50 µl of virus suspension to the pre-incubated cells. Virus control wells (n = 6) received 50 µl of test medium and 50 µl of virus suspension. The multiplicity of infection (MOI) was published [30]. Cell control wells (n = 6) were inoculated with 100 µl of test medium. After observing a complete cytopathic effect in virus control wells under a light microscope at day 3 p.i., cells were fixed, stained, and de-stained for optical density determination and calculation of the percentage of CPE inhibition as published [32]. At least 4 independent experiments were performed (single measurement per single concentration or combination). The results were used as replicates to calculate the mean, standard deviation, and 95 % confidence intervals (95 % CI) for the percentage of CPE inhibition during analysis of drug combination data using SynergyFinder Plus [47].

Linear regression analysis using Microsoft Excel was applied in the linear scaled dose-dependent sample concentrations to calculate the IC_{50} values of pleconaril and OBR-5–340 monotherapy.

2.3. Analysis of drug combination data

Expected drug combination responses, 95 % CI, and p values were calculated based on Loewe, Bliss, ZIP, and HAS reference models using SynergyFinder Plus [47]. Generally, deviations between observed and expected responses with positive and negative values denote synergy and antagonism, respectively. For example synergy score of 15 corresponds to 15 % of response beyond expectation. There is no particular threshold to define a good synergy score. According to Tang et al. consistency between different reference models should be indicative for the degree in synergy [37]. If different models classify a combination of drugs as synergistic, synergism is called strong. In case of weak synergy, the combination is classified as synergistic to one model only.

Pearsońs correlation coefficients were calculated with EXCEL2016.

2.4. Molecular dynamic simulations

We performed molecular dynamic simulations to explain the origin of synergistic effect. To reflect diversity of binding sensitivity, we selected 5 capsid proteins from RV types from different groups, sensitive or insensitive to pleconaril and/or OBR-5–340 (summarized in paragraph 2.1). Those are proteins from RV-B5, RV-A8, RV-B52, RV-A2 and RV-B3. Coordinates of heavy atoms of the RV-B5 complex with the OBR-5–340 were taken from the cryo-EM structure, **PDB ID: 6SK5** [43]. Proteins from other RV-B type were obtained from the same structure, introducing amino acid substitutions according to [21]. Similarly, capsid proteins from RV-A type were obtained from the crystal structure of the RV-A16 capsid protein, **PDB ID: 1C8M**. Thus, we examined formation of triple complexes of protein with both compounds, OBR-5–340 and pleconaril. We started with structures with the positions of inhibitors mimicking binary complexes of each inhibitor with the protein and analyzed the finally formed stable complexes. Additional model was prepared for a binary complex of the RV-A16 capsid protein with pleconaril to verify the model on the binary complex that is known to be stable according to our previous studies [30].

MD simulations were performed as follows: 50 ns system equilibration with the following 400 ns production run for each model system. Protein macromolecule was described with CHARMM36 force field parameters [4,5], OBR-5–340 and pleconaril with the CGenFF [41] and solvent water molecules with the TIP3P [17] parameters. Simulations were performed in the NPT ensemble at T = 300 K and p = 1 atm with the 1 fs integration time step. All MD simulations were carried out with the NAMD software package [28]. Dynamical network analysis [34] was utilized to divide the complex to communities with the correlated motions within them. To do this, every amino acid was represented by a single node. The OBR-5–340, and pleconaril molecules were divided into three nodes. Any two nodes (except the neighbors) were connected by an edge if the distance between any pair of atoms of the respective residues was less than 4 Å for more than 75 % of the simulation time. Covariance and correlation matrices for dynamical network analysis were calculated with the Carma program [9].

3. Results

3.1. Drug combination studies revealed synergistic interactions of OBR-5–340 and pleconaril

The IC_{50} values and dose response curves of monotherapy with pleconaril and OBR-5–340 were summarized in Supplementary Table 2 and Supplementary Material 1–9, respectively. As shown before [21,25], RV-B5, RV-B48, and RV-B69 were insensitive to pleconaril, but highly sensitive to OBR-5–340 (IC_{50} between 0.13 and 0.61 µM). RV-A8, RV-B17, and RV-B52 were sensitive to pleconaril (IC_{50} between 0.99 and 5.37 µM; the IC_{50} value of 0.99 µM pleconaril to RV-B17 was borderline) and OBR-5–340 (IC_{50} between 12.56 and 17.25 µM). In contrast, RV-A2, RV-B3, and RV-B70 represent highly pleconaril sensitive (IC_{50} between 0.02 and 0.36 µM), OBR-5–340 sensitive (IC_{50} between 8.89 and 17.81 µM) RV types. Thus, our screening platform included three sets of RV types with distinct sensitivities to pleconaril and OBR-5–340.

Dose-response matrixes (mean percentage of CPE inhibition with SD) of all inhibitor combinations and RV types are summarized in Fig. 2. In addition, the mean percentage of CPE inhibition with 95 % CI are part of the Synergy Finder Plus reports (Supplementary Material 1–9). The dose-response matrixes provided the basis for calculations of synergy scores with 95 % CI (Supplementary Material 1–9), 2D surface plots (Figs. 3–5) as well as mean synergy scores and p values (Supplementary Table 3).

To reduce the risk of methodological bias, synergism analysis was performed for all RV types using Loewe, Bliss, ZIP, and HSA reference models. The mean synergy scores of Bliss and ZIP models matched best (Pearsońs of 0.997). Higher mean synergy scores were calculated with Loewe and/or HSA model compared to Bliss and ZIP models. The mean synergy scores calculated with Loewe did strongly correlate with that from HSA model (Pearsońs of 0.993) but not with that from Bliss and ZIP model (Pearsońs of −0.076 and −0.256). In contrast, the mean synergy scores calculated with HSA correlated well with that calculated with Bliss and ZIP (Pearsońs of 0.986 and 0.983, respectively).

At certain concentrations, synergy scores indicated strong antagonistic interactions (dark green in Figs. 3–5) with synergy score less than −10 (Supplementary material 1–9). Strong antagonism was detected in all reference models when (i) pleconaril concentrations equal or higher than 4.38 µM (RV-B48), 8.75 (RV-B69) or 17.5 µM (RV-B5) and/or (ii) concentration of 70 µM of OBR-5–340 (RV-A2 and RV-B3) were combined. In addition, a synergy score less than −10 was calculated with ZIP and Bliss models for RV-A8, RV-B17, RV-B52, RV-B70 when 70 µM of OBR-5–340 were combined with certain pleconaril concentration. These results show an impact of the RV type studied on synergy. In addition, monotherapies were non-cytotoxic, but combinations could still interact differently. Therefore, future experiments will directly validate cytotoxicity at combination doses.

The comparison of synergistic scores of most synergistic areas colored in red tones further confirmed the impact of the RV type studied on synergy (Figs. 3–5 and Supplementary Material 1–9). They revealed a moderate potentiation of CPE inhibition for the pleconaril-insensitive, highly OBR-5–340-sensitive RV-B5, RV-B48, and RV-B69 at certain inhibitor combinations (areas colored in light red and red in Fig. 3). Areas indicating a strong synergism with synergistic scores higher than 10 were identified for all pleconaril- and OBR-5–340-sensitive RV types as

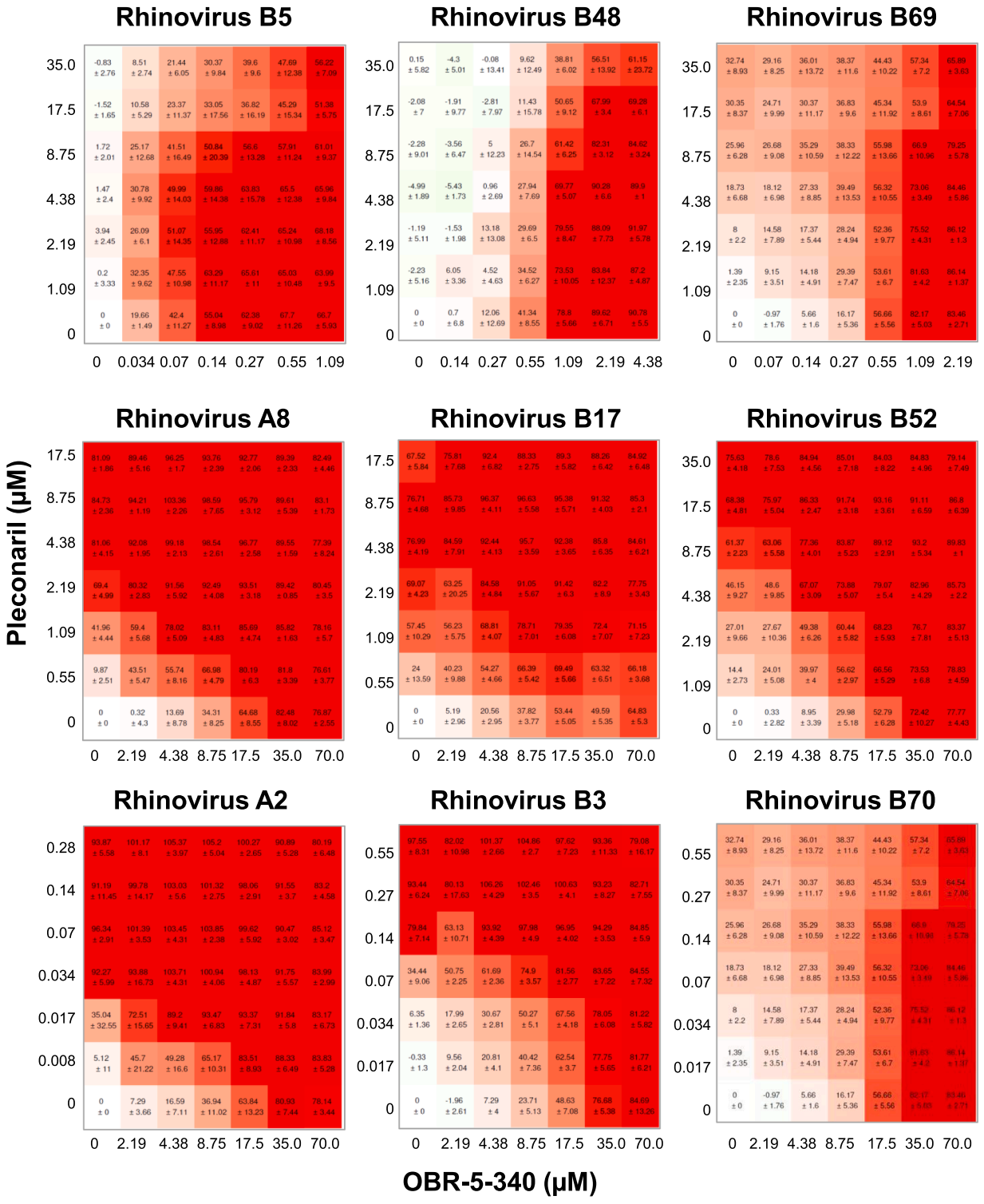

Fig. 2. Dose-response matrixes for pleconaril-OBR-5–340 combinations and 9 rhinoviruses, insensitive or sensitive to the inhibitors in monotherapy. The antiviral activity was analyzed in least 4 independent cytopathic effect (CPE) inhibition assays in HeLa cells. The results were used as replicates to calculate the mean percentage of CPE inhibition and standard deviations with SyngeryFinder Plus.

well as highly pleconaril-sensitive, OBR-5–340-sensitive RV types with the 4 reference models (Figs. 4 and 5). Hence, pleconaril+OBR-5–340 combinations clearly outperformed monotherapy at certain concentrations.

3.2. *Molecular dynamic simulations explain the origin of synergistic effect*

Protein-pleconaril complexes have not been studied before, therefore, we also simulated the dynamic behavior of the capsid protein from the insensitive RV-B5 and sensitive RV-A16 strains. In our previous study [30] we demonstrated that binding efficiency of the OBR-5–340 and other compounds with the same core is determined by the collective

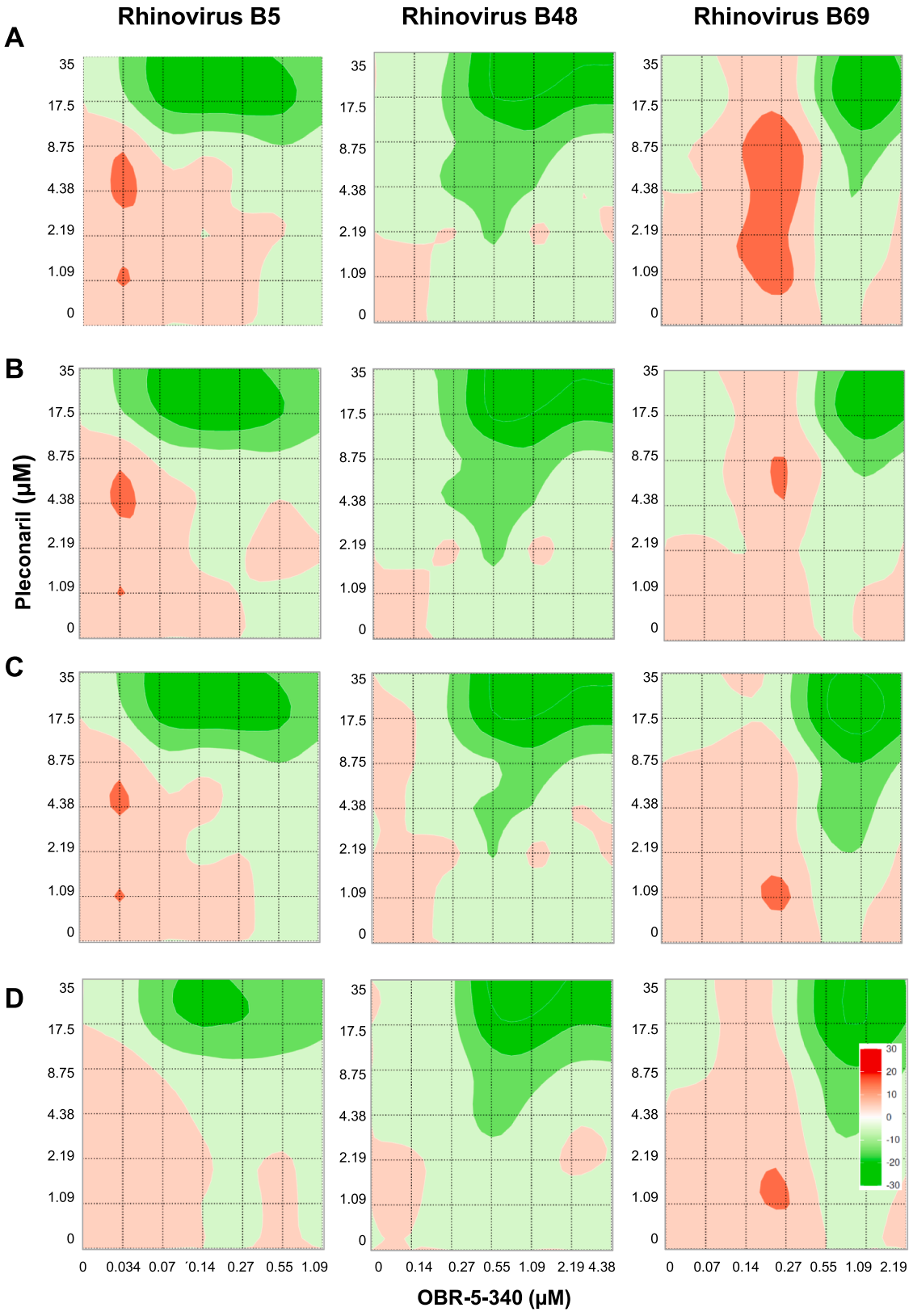

Fig. 3. Synergy interaction landscapes of pleconaril-OBR-5–340 combinations and RV-B5, RV-B48, and RV-B69 in HeLa Ohio cells. Cells were treated with single inhibitor or inhibitor combinations and infected with the respective RV type or mock for 72 h. Thereafter, cell viability was measured to calculate synergy scores using (A) HSA, (B) Loewe, (C) Bliss, and (D) ZIP models. The data of four independent experiments were used as replicates for synergism analysis with SynergyFinder Plus. Antagonistic and synergistic score areas are colored in green or red tones, respectively. At certain concentrations, synergy scores less than −10 indicated strong antagonistic interactions (green and dark green) for RV-B5, RV-B48, and RV-B69 in all reference models. A moderate potentiation of CPE inhibition was also found at certain inhibitor combinations (areas colored in light red and red with synergy score between 0 and 10 or >10, respectively) for these RV types in all reference models.

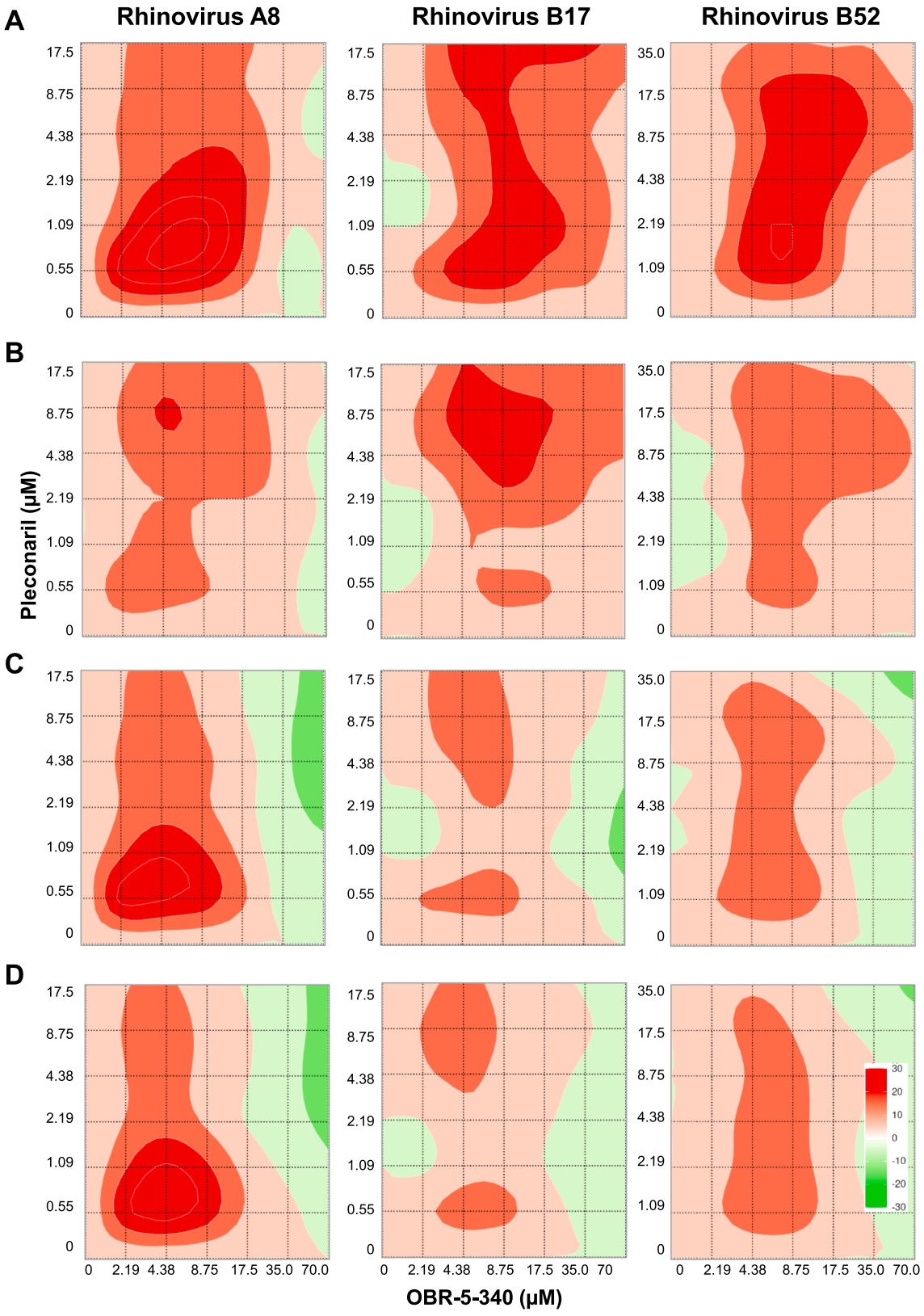

Fig. 4. Synergy interaction landscapes for pleconaril-OBR-5–340 combinations and RV-A8, RV-B17, and RV-B52 in HeLa Ohio cells. Cells were treated with single inhibitor or inhibitor combinations and infected with the respective RV or mock for 72 h. Thereafter, cell viability was measured to calculate synergy scores using (A) HSA, (B) Loewe, (c) Bliss, and (C) ZIP models. The data of four independent experiments were used as replicates for synergism analysis with SynergyFinder Plus. Antagonistic and synergistic score areas are colored in green or red tones, respectively. Small areas indicating a strong antagonism (synergy scores less than −10; green color) were detected for RV-A8 and RV-B52 with Bliss and ZIP models (C and D) and RV-B17 with Bliss model at high OBR-5–340 certain concentrations. In contrast, large red or even dark red areas (synergistic scores higher than 10 or 20, respectively) showstrong synergistic interactions for these three pleconaril- and OBR-5–340-sensitive RV types with all reference models.

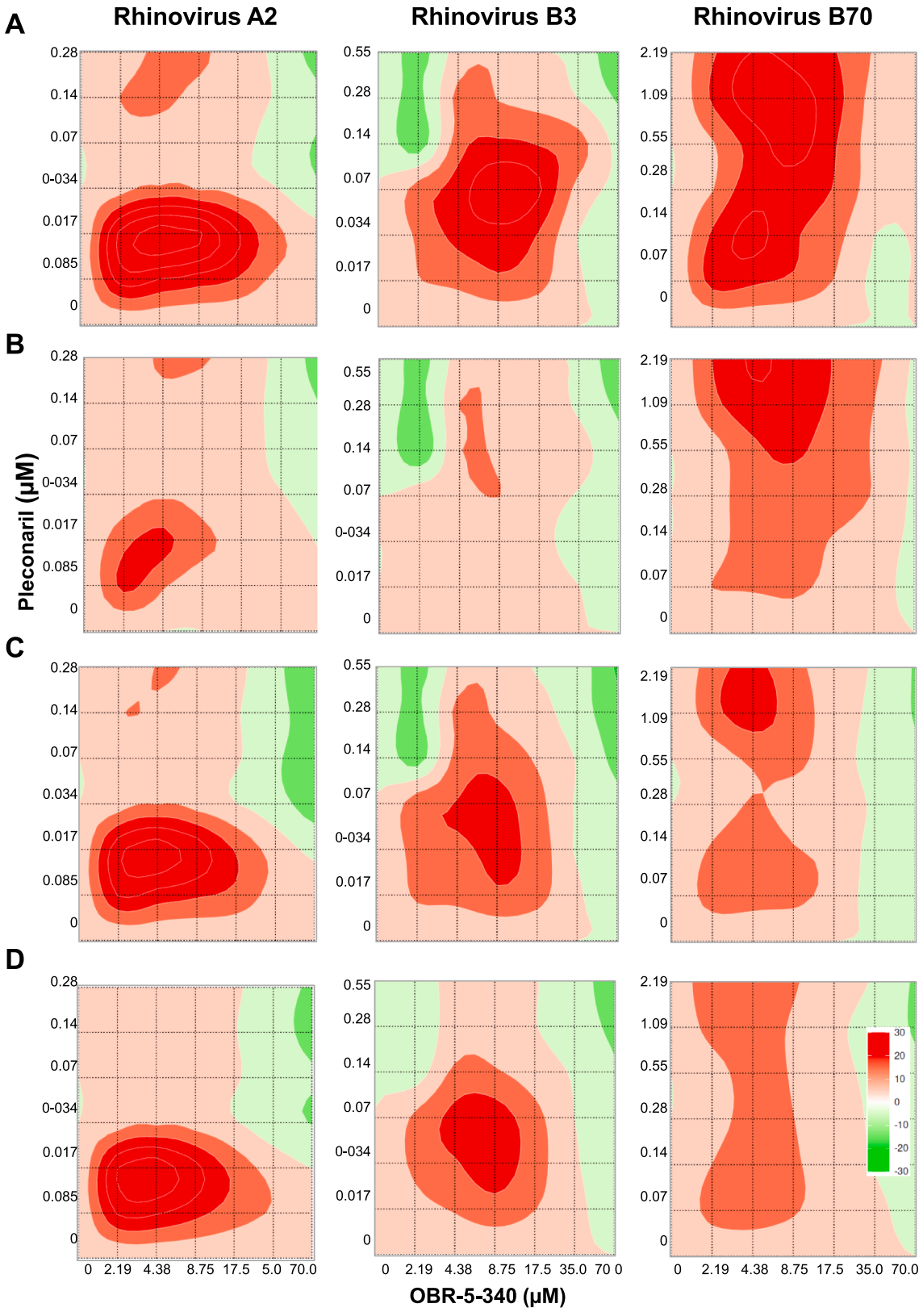

Fig. 5. Synergy interaction landscapes for pleconaril-OBR-5–340 combinations and RV-A2, RV-B3, and RV-B70 in HeLa Ohio cells. Cells were treated with single inhibitor or inhibitor combinations and infected with the respective RV or mock for 72 h. Thereafter, cell viability was measured to calculate synergy scores using (A) HSA, (B) Loewe, (c) Bliss, and (C) ZIP models. The data of four independent experiments were used as replicates for synergism analysis with SynergyFinder Plus. Antagonistic and synergistic score areas are colored in green or red tones, respectively. Small areas indicating a strong antagonism (synergy scores less than −10; green color) were detected for RV-A2 and RV-B3 with all reference models and for RV-B70 with Bliss and ZIP models (C and D) in particular when 70 μM of OBR-5–340 were combined. In contrast, large red or even dark red areas (synergistic scores higher than 10 or 20, respectively) demonstrate strong synergistic interactions for these three pleconaril- and OBR-5–340-sensitive RV types with all reference models.

motions of the inhibitor and the protein loops that envelope it. We performed similar simulations for complexes with pleconaril to evaluate binding affinity and transferability of the suggested methodology here. In complex with A16 (good binding affinity) we observed the same collective motion as for the OBR-5–340 series that we postulated earlier [30]. This allows us to generalize the model and prove that the collective motion of the loops enveloping the capsid binder indeed determines binding affinity.

Molecular dynamic simulations for all considered systems revealed that the triple complexes including VP1, pleconaril, and OBR-5–340 are stable with respect to the interactions between two capsid binders (Fig. 6). Pleconaril occupies the same binding site as in the binary complex and OBR-5–340 binds near to the entrance of the hydrophobic pocket in VP1 representing the binding site of pleconaril (Fig. 6A, B). The complex of the two capsid binders mimics an "elongated" molecule formed due to non-covalent interactions between pleconaril and OBR-5–340 (Fig. 6C). Importantly, the binding of both molecules does not disturb the loops at the entrance of the binding site. The distance between the main chains of these loops becomes only about 1 Å larger.

4. Discussion

The monotherapy results fully confirmed the previously published inhibitory profile of two capsid binder's pleconaril and OBR-5–340 against the RV types sets of the screening platform [21,25]. Each three RV types were: (i) pleconaril-insensitive, highly OBR-5–340-sensitive, (ii) pleconaril- and OBR-5–340-sensitive, or (iii) highly pleconaril-sensitive, OBR-5–340-sensitive. This enabled us to consider the distinct sensitivity profiles of multiple RV types (based on VP1 variability) to both capsid binders in the interaction of the compounds.

A high concentration range of pleconaril and OBR-5–340 was tested. In accordance with a methodical paper published by Vlot et al. [42], concentrations lower and higher than published IC_{50} values [21,25] were included. After oral application, a maximum plasma concentrations of 1.25 μg/ml OBR-5–340 (3.39 μM) was measured in preclinical studies in mice ([25]; 100 mg/kg). The maximum plasma concentration of pleconaril was 3.14 μg/ml (8.23 μM) in mice ([27]; 200 mg/kg) and 2.34 μg/ml (6.14 μM) in adults [1,2]; 400 mg per os). Hence, for some RV types the maximal tested concentrations were higher than the previously determined maximal plasma concentrations after oral application. However, anti-RV drugs might also be administered topically e.g. as drops or spray. Given the low systemic absorption with topical formulations, higher local drug concentrations might be achieved, potentially mitigating the plasma concentration limitations observed with oral administration.

The concentrations used in our combination study were well tolerated in monotherapy in HeLa cells [25]. However, we cannot fully exclude that an enhanced cytotoxicity contributes to the antagonistic effects seen in combinations with 70 μM OBR-5–340. To clarify this, cytotoxicity combination studies will be included in ongoing preclinical studies for clarification.

Our primary hypothesis concerning the observed antagonism in certain pleconaril-OBR-5–340 combinations is founded on the binding dynamics of both inhibitors to VP1. It is hypothesized that a ternary complex is formed if pleconaril binds into the hydrophobic pocket of VP1 before OBR-5–340 binds near to the pocket entrance. In the event of excess of OBR-5–340, this may impede the penetration of pleconaril into the canyon, thereby antagonizing ternary complex formation in both pleconaril- and OBR-5–340-sensitive RV types. In contrast, excess pleconaril prevented OBR-5–340 binding and thus ternary complex formation in RV types that were insensitive to pleconaril and highly sensitive to OBR-5–340.

Our study results are the first to demonstrate synergistic combinations of two broad-spectrum capsid binders of RV types. Other groups have focused on combinations of broad-spectrum anti-enteroviral agents acting against different targets, for example the viral capsid and protease (e.g. pleconaril or vapendavir combined with rupintrivir) or the viral capsid and polymerase (e.g. pleconaril or vapendavir combined with enviroxime or remdesivir). The results demonstrated additive to synergistic interactions of pleconaril-rupintrivir [14], pleconaril-enviroxime [12], vapendavir-rupintrivir, and vapendavir-enviroxime [40] combinations. Investigating the combinatorial effects of two broad-spectrum capsid binders that both fit into the highly conserved hydrophobic pocket in VP1 (pleconaril and vapendavir) Ianevski et al. showed additive effects against echovirus 1 [12]. In contrast, novel synergistic combinations of two capsid binders were identified here.

Different reference models confirmed these results. In agreement with observations of other groups from anti-cancer research [8,42], the

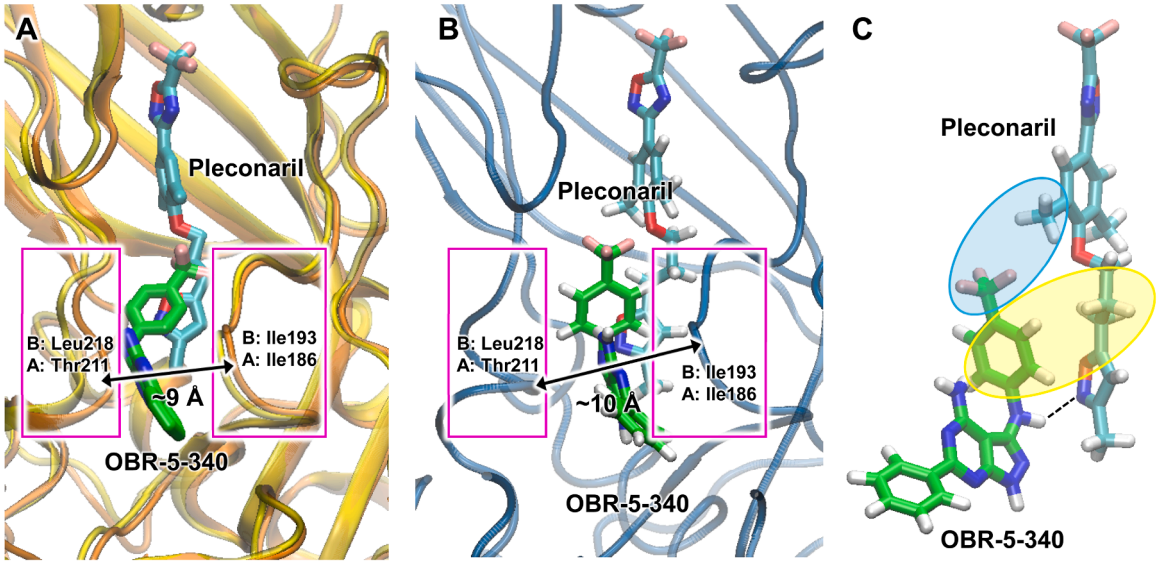

Fig. 6. (A) Alignment of experimental structures of the capsid protein of RV-A16 (yellow) with pleconaril (cyan), PDB ID: 1C8M, and capsid protein of RV-B5 (orange) with OBR-5–340 (green), PDB ID: 6SK5. Loops, enveloping the OBR-5–340 binding site are highlighted by magenta squares. Interatomic distances are measured between CA atoms of residues of these loops. A and B in the notation correspond to the RV-A and RV-B types. (B) Representative structure of the triple complex of RV-B52 capsid protein, pleconaril and OBR-5–340. (C) Interacting regions of the inhibitor molecule. Dashed line corresponds to the hydrogen bond, hidrophobic interactions are highlighted in yellow, interactions of -CF_3 and -CH_3 groups are blue.

synergy scores varied between the models and thus further confirmed that the choice of a synergy model could influence the synergy score [8,42,44]. As found in a combination study with anticancer drugs, [45] the mean synergistic area scores calculated with Loewe did not correlate well with that from Bliss and ZIP models here. The strong dependence of the accuracy of Loewe on both the same maximum response and constant potency ratio of the combined inhibitors [42,45] might explain these results. The higher synergy scores calculated with HSA might be due to the lower threshold of this model for assigning synergy compared to other methods [45]. Albeit being a hybrid model of Loewe and Bliss, the ZIP model is independent from assumptions considering the PK/PD profile of the compounds in combination [42,45]. In summary, the general conclusions on potentiation and/or synergism drawn from our combination screen with the different reference models are similar, whereat the results from Bliss independence and ZIP models being the most consistent in our context.

Whereas pleconaril binds deep into the hydrophobic pocket of VP1 of RV A and B types [46] OBR-5–340 interacts with amino acids close to the entrance of this pocket [43]. Both compounds interact with VP1 by non-covalent way in monotherapy [22,43]. We hypothesized that the coincident binding of both capsid binders to VP1 might lead to faster and/or stronger effects on the viral capsid at certain concentrations what might explain the demonstrated synergism. This occurs due to the formation of the triple complex. Non-covalent interactions (hydrophobic and H-bonds) stabilize the ternary complex. Typically, non-covalent binding results in the formation of complexes that exhibit significantly weaker binding affinities than covalent binding. We suggest that the formation of a ternary complex with non-covalent binding of two molecules to VP1 ensures the stability of the resulting complex. This is close to covalent binding in terms of stability. Likely, the magnitude of the synergistic effect is determined by the interplay of the binding constants. Importantly, the binding of two molecules does not disturb the binding site including the loops at the entrance that were found to be important for binding [30]. Fig. 5 allows us to hypothesize that the synergistic effect starts to be pronounced after pleconaril binding. The synergistic area is gradually shifted to higher pleconaril concentrations in line of capsid proteins from RV-A2, RV-B3, RV-B70. This is consistent with the gradual increase of the IC_{50} value [30] in the same line: 0.05 μM for RV-A2, 0.12 μM for RV-B3 and 0.4 μM for RV-B70. Taken together, the study results confirm the hypothesis that pleconaril and OBR-5–340 can bind simultaneously to VP1 thereby inhibiting a broader spectrum of RV types. Moreover, the formation of a triple helix between VP1, pleconaril, and OBR-5–340 leads to significant synergistic effects of pleconaril-OBR-5–340 combinations at specific concentration ranges for multiple RV types.

We are aware that our study has some limitations. While we observed no significant cytotoxicity in monotherapy [25], it is important to conduct cytotoxicity combination studies. The results could clarify whether certain pleconaril-OBR-5–340 combinations affect cytotoxicity and thus contribute to antagonism. Moreover, studies with further RV types, respiratory cell lines (e.g. A549 and Calu 3) or even organoid cultures would increase the generalizability of our studies results. In addition, cryo electron microscopy could be used to visualize the simultaneous binding of both capsid-binding inhibitors to VP1.

In summary, our findings contribute to the development of broader-spectrum anti-RV or even anti-enterovirus treatment. Both inhibitors can be co-administered orally. That is an advantage for their use in patients. The inclusion of a third inhibitor could further improve the treatment effect. Further steps for translating our findings into *in vivo,* human challenge or clinical studies are experiments in respiratory cells or lung organoids aiming to confirm the synergism under more natural conditions. In addition, other clinically relevant respiratory enteroviruses e.g. enterovirus 71 and D68 should by included. Experiments on the evolution of drug resistance in response to combination treatment will get insights into long-term antiviral efficacy. Pharmacokinetic modelling in an animal model would further help bridge the gap between in vitro and potential clinical applications.

5. Conclusions

The present study contributes to the ongoing efforts to develop medications for the treatment of RV infections. Using pleconaril and OBR-5–340 as examples, we have shown for multiple RV types with different sensitivity to both inhibitors that combinations of two broad-spectrum capsid binders can significantly enhance the treatment effect. The potency and/or efficacy were enhanced at concentrations that were reported in pharmacokinetic study reports *in vivo* and/or in humans [1,2,25,27]. Therefore, such synergistic capsid binder combinations have the potential to improve treatment efficacy. Additionally, they will better address a major challenge of drug development – efficacy against almost all RV-A and RV-B types circulating throughout the year.

The formation of a triple complex of VP1, pleconaril, and OBR-5–340 explains the strong synergistic interactions observed. After binding of pleconaril into the hydrophobic pocket of VP1, OBR-5–340 binds to the entrance of VP1 and both capsid binders mimics an “elongated” inhibitor molecule.

The strong synergistic interactions between pleconaril and OBR-5–340, mediated through simultaneous binding to VP1, provide a promising platform for the future development of combination therapies against rhinovirus and other enteroviruses. In preclinical studies (i) the synergism, (ii) (lower) dosing, (iii) reduced risk of resistance evolution should be confirmed in organoid cultures and the human challenge model. The oral co-administration of pleconaril and OBR-5–340 is an advantage for their use in patients. Moreover, our findings suggest a double positive effect on patients. On the one hand infections with more RV types can be treated. On the other hand, there will be a stronger antiviral activity against each individual RV type. In this way, patients are benefitted from easy medication intake and better therapeutic success.

CRediT authorship contribution statement

Maria Khrenova: Writing – review & editing, Writing – original draft, Visualization, Validation, Methodology, Investigation, Formal analysis, Data curation, Conceptualization. **Martina Richter:** Validation, Methodology, Investigation, Data curation, Conceptualization. **Michaela Schmidtke:** Writing – original draft, Visualization, Validation, Supervision, Project administration, Formal analysis, Data curation, Conceptualization. **Vadim Makarov:** Writing – review & editing, Writing – original draft, Visualization, Validation, Supervision, Project administration, Funding acquisition, Formal analysis, Data curation. **Olga Riabova:** Methodology, Funding acquisition, Formal analysis, Data curation.

Grants/funding

This research did not receive any specific grant from funding agencies in the public, commercial, or not-for-profit sectors.

Patents

50 2007 006 042.9
50 2012 017 045.1

Declaration of Competing Interest

The authors declare the following financial interests/personal relationships which may be considered as potential competing interests:

Acknowledgements

We thank Birgit Jahn for technical support. The Russian Science Foundation (project number 24-15-00066) supported OR and VM.

Appendix A. Supporting information

Supplementary data associated with this article can be found in the online version at doi:10.1016/j.biopha.2025.118193.

Data availability

Data will be made available on request.

References

[1] S.M. Abdel-Rahman, G.L. Kearns, Single-dose pharmacokinetics of a pleconaril (VP63843) oral solution and effect of food, Antimicrob. Agents Chemother. 42 (1998) 2706–2709.
[2] S.M. Abdel-Rahman, G.L. Kearns, Single oral dose escalation pharmacokinetics of pleconaril (VP 63843) capsules in adults, J. Clin. Pharm. 39 (1999) 613–618.
[3] R. Abdelnabi, J.A. Geraets, Y. Ma, C. Mirabelli, J.W. Flatt, A. Domanska, L. Delang, D. Jochmans, T.A. Kumar, V. Jayaprakash, B.N. Sinha, P. Leyssen, S.J. Butcher, J. Neyts, A novel druggable interprotomer pocket in the capsid of rhino- and enteroviruses, PLoS Biol. 17 (2019) e3000281.
[4] R.B. Best, X. Zhu, J. Shim, P.E. Lopes, J. Mittal, M. Feig, A.D. Mackerell Jr., Optimization of the additive CHARMM all-atom protein force field targeting improved sampling of the backbone phi, psi and side-chain chi(1) and chi(2) dihedral angles, J. Chem. Theory Comput. 8 (2012) 3257–3273.
[5] E.J. Denning, U.D. Priyakumar, L. Nilsson, A.D. Mackerell Jr., Impact of 2′-hydroxyl sampling on the conformational properties of RNA: update of the CHARMM all-atom additive force field for RNA, J. Comput. Chem. 32 (2011) 1929–1943.
[6] A. Egorova, S. Ekins, M. Schmidtke, V. Makarov, Back to the future: Advances in development of broad-spectrum capsid-binding inhibitors of enteroviruses, Eur. J. Med. Chem. 178 (2019) 606–622.
[7] C. Esneau, A.C. Duff, N.W. Bartlett, Understanding Rhinovirus Circulation and Impact on Illness, Viruses 14 (2022).
[8] J. Foucquier, M. Guedj, Analysis of drug combinations: current methodological landscape, Pharm. Res. Perspect. 3 (2015) e00149.
[9] N.M. Glykos, Software news and updates. Carma: a molecular dynamics analysis program, J. Comput. Chem. 27 (2006) 1765–1768.
[10] F.G. Hayden, D.T. Herrington, T.L. Coats, K. Kim, E.C. Cooper, S.A. Villano, S. Liu, S. Hudson, D.C. Pevear, M. Collett, M. McKinlay, G. Pleconaril Respiratory Infection Study, Efficacy and safety of oral pleconaril for treatment of colds due to picornaviruses in adults: results of 2 double-blind, randomized, placebo-controlled trials, Clin. Infect. Dis. 36 (2003) 1523–1532.
[11] T. Heikkinen, A. Jarvinen, The common cold, Lancet 361 (2003) 51–59.
[12] A. Ianevski, I.T. Froysa, H. Lysvand, C. Calitz, T. Smura, H.J. Schjelderup Nilsen, E. Hoyer, J.E. Afset, A. Sridhar, K.C. Wolthers, E. Zusinaite, T. Tenson, R. Kurg, V. Oksenych, A.S. Galabov, A. Stoyanova, M. Bjoras, D.E. Kainov, The combination of pleconaril, rupintrivir, and remdesivir efficiently inhibits enterovirus infections in vitro, delaying the development of drug-resistant virus variants, Antivir. Res. 224 (2024) 105842.
[13] A. Ianevski, A.K. Giri, T. Aittokallio, SynergyFinder 3.0: an interactive analysis and consensus interpretation of multi-drug synergies across multiple samples, Nucleic Acids Res. 50 (2022) W739–W743.
[14] A. Ianevski, E. Zusinaite, T. Tenson, V. Oksenych, W. Wang, J.E. Afset, M. Bjoras, D.E. Kainov, Novel synergistic anti-enteroviral drug combinations, Viruses (2022) 14.
[15] D.J. Jackson, J.E. Gern, Rhinovirus infections and their roles in asthma: etiology and exacerbations, J. Allergy Clin. Immunol. Pract. 10 (2022) 673–681.
[16] S.E. Jacobs, D.M. Lamson, K. St George, T.J. Walsh, Human rhinoviruses, Clin. Microbiol. Rev. 26 (2013) 135–162.
[17] W.L. Jorgensen, J. Chandrasekhar, J.D. Madura, R.W. Impey, M.L. Klein, Comparison of simple potential functions for simulating liquid water, J. Chem. Phys. 79 (1983) 926–935.
[18] L. Kaiser, C.E. Crump, F.G. Hayden, In vitro activity of pleconaril and AG7088 against selected serotypes and clinical isolates of human rhinoviruses, Antivir. Res. 47 (2000) 215–220.
[19] G.L. Kearns, S.M. Abdel-Rahman, L.P. James, D.L. Blowey, J.D. Marshall, T. G. Wells, R.F. Jacobs, Single-dose pharmacokinetics of a pleconaril (VP63843) oral solution in children and adolescents, Pediatr. Pharmacol. Res. Unit. Netw. Antimicrob. Agents Chemother. 43 (1999) 634–638.
[20] R.M. Ledford, M.S. Collett, D.C. Pevear, Insights into the genetic basis for natural phenotypic resistance of human rhinoviruses to pleconaril, Antivir. Res. 68 (2005) 135–138.
[21] R.M. Ledford, N.R. Patel, T.M. Demenczuk, A. Watanyar, T. Herbertz, M.S. Collett, D.C. Pevear, VP1 sequencing of all human rhinovirus serotypes: insights into genus phylogeny and susceptibility to antiviral capsid-binding compounds, J. Virol. 78 (2004) 3663–3674.
[22] Y. Liu, J. Sheng, A. Fokine, G. Meng, W.H. Shin, F. Long, R.J. Kuhn, D. Kihara, M. G. Rossmann, Structure and inhibition of EV-D68, a virus that causes respiratory illness in children, Science 347 (2015) 71–74.
[23] J.D. Ma, A.N. Nafziger, G. Rhodes, S. Liu, J.S. Bertino Jr., Duration of pleconaril effect on cytochrome P450 3A activity in healthy adults using the oral biomarker midazolam, Drug Metab. Dispos. 34 (2006) 783–785.
[24] J.D. Ma, A.N. Nafziger, G. Rhodes, S. Liu, A.M. Gartung, J.S. Bertino Jr., The effect of oral pleconaril on hepatic cytochrome P450 3A activity in healthy adults using intravenous midazolam as a probe, J. Clin. Pharm. 46 (2006) 103–108.
[25] V.A. Makarov, H. Braun, M. Richter, O.B. Riabova, J. Kirchmair, E.S. Kazakova, N. Seidel, P. Wutzler, M. Schmidtke, Pyrazolopyrimidines: potent inhibitors targeting the capsid of rhino- and enteroviruses, ChemMedChem 10 (2015) 1629–1634.
[26] D.C. Pevear, F.G. Hayden, T.M. Demenczuk, L.R. Barone, M.A. McKinlay, M. S. Collett, Relationship of pleconaril susceptibility and clinical outcomes in treatment of common colds caused by rhinoviruses, Antimicrob. Agents Chemother. 49 (2005) 4492–4499.
[27] D.C. Pevear, T.M. Tull, M.E. Seipel, J.M. Groarke, Activity of pleconaril against enteroviruses, Antimicrob. Agents Chemother. 43 (1999) 2109–2115.
[28] J.C. Phillips, D.J. Hardy, J.D.C. Maia, J.E. Stone, J.V. Ribeiro, R.C. Bernardi, R. Buch, G. Fiorin, J. Henin, W. Jiang, R. McGreevy, M.C.R. Melo, B.K. Radak, R. D. Skeel, A. Singharoy, Y. Wang, B. Roux, A. Aksimentiev, Z. Luthey-Schulten, L. V. Kale, K. Schulten, C. Chipot, E. Tajkhorshid, Scalable molecular dynamics on CPU and GPU architectures with NAMD, J. Chem. Phys. 153 (2020) 044130.
[29] M. Richter, K. Doring, D. Blaas, O. Riabova, M. Khrenova, E. Kazakova, A. Egorova, V. Makarov, M. Schmidtke, Molecular mechanism of rhinovirus escape from the Pyrazolo[3,4-d]pyrimidine capsid-binding inhibitor OBR-5-340 via mutations distant from the binding pocket: derivatives that brake resistance, Antivir. Res. 222 (2024) 105810.
[30] M. Richter, M. Khrenova, E. Kazakova, O. Riabova, A. Egorova, V. Makarov, M. Schmidtke, Dynamic features of virus protein 1 and substitutions in the 3-phenyl ring determine the potency and broad-spectrum activity of capsid-binding pyrazolo[3,4-d]pyrimidines against rhinoviruses, Antivir. Res. 231 (2024) 105993.
[31] J.M. Rollinger, M. Schmidtke, The human rhinovirus: human-pathological impact, mechanisms of antirhinoviral agents, and strategies for their discovery, Med. Res. Rev. 31 (2011) 42–92.
[32] M. Schmidtke, U. Schnittler, B. Jahn, H. Dahse, A. Stelzner, A rapid assay for evaluation of antiviral activity against coxsackie virus B3, influenza virus A, and herpes simplex virus type 1, J. Virol. Methods 95 (2001) 133–143.
[33] K. Senior, FDA panel rejects common cold treatment, Lancet Infect. Dis. 2 (2002) 264.
[34] A. Sethi, J. Eargle, A.A. Black, Z. Luthey-Schulten, Dynamical networks in tRNA: protein complexes, Proc. Natl. Acad. Sci. USA 106 (2009) 6620–6625.
[35] Z.A. Shyr, Y.S. Cheng, D.C. Lo, W. Zheng, Drug combination therapy for emerging viral diseases, Drug Discov. Today 26 (2021) 2367–2376.
[36] P. Simmonds, A.E. Gorbalenya, H. Harvala, T. Hovi, N.J. Knowles, A.M. Lindberg, M.S. Oberste, A.C. Palmenberg, G. Reuter, T. Skern, C. Tapparel, K.C. Wolthers, P. C.Y. Woo, R. Zell, Recommendations for the nomenclature of enteroviruses and rhinoviruses, Arch. Virol. 165 (2020) 793–797.
[37] J. Tang, K. Wennerberg, T. Aittokallio, What is synergy? The Saariselka agreement revisited, Front. Pharm. 6 (2015) 181.
[38] S. Taylor, P. Lopez, L. Weckx, C. Borja-Tabora, R. Ulloa-Gutierrez, E. Lazcano-Ponce, A. Kerdpanich, M. Angel Rodriguez Weber, A. Mascarenas de Los Santos, J. C. Tinoco, M.A. Safadi, F.S. Lim, M. Hernandez-de Mezerville, I. Faingezicht, A. Cruz-Valdez, Y. Feng, P. Li, S. Durviaux, G. Haars, S. Roy-Ghanta, D.W. Vaughn, T. Nolan, Respiratory viruses and influenza-like illness: epidemiology and outcomes in children aged 6 months to 10 years in a multi-country population sample, J. Infect. 74 (2017) 29–41.
[39] H.J. Thibaut, C. Lacroix, A.M. De Palma, D. Franco, M. Decramer, J. Neyts, Toward antiviral therapy/prophylaxis for rhinovirus-induced exacerbations of chronic obstructive pulmonary disease: challenges, opportunities, and strategies, Rev. Med. Virol. 26 (2016) 21–33.
[40] H.J. Thibaut, P. Leyssen, G. Puerstinger, A. Muigg, J. Neyts, A.M. De Palma, Towards the design of combination therapy for the treatment of enterovirus infections, Antivir. Res. 90 (2011) 213–217.
[41] K. Vanommeslaeghe, E. Hatcher, C. Acharya, S. Kundu, S. Zhong, J. Shim, E. Darian, O. Guvench, P. Lopes, I. Vorobyov, A.D. Mackerell Jr., CHARMM general force field: a force field for drug-like molecules compatible with the CHARMM all-atom additive biological force fields, J. Comput. Chem. 31 (2010) 671–690.
[42] A.H.C. Vlot, N. Aniceto, M.P. Menden, G. Ulrich-Merzenich, A. Bender, Applying synergy metrics to combination screening data: agreements, disagreements and pitfalls, Drug Discov. Today 24 (2019) 2286–2298.
[43] J. Wald, M. Pasin, M. Richter, C. Walther, N. Mathai, J. Kirchmair, V.A. Makarov, N. Goessweiner-Mohr, T.C. Marlovits, I. Zanella, A. Real-Hohn, N. Verdaguer, D. Blaas, M. Schmidtke, Cryo-EM structure of pleconaril-resistant rhinovirus-B5 complexed to the antiviral OBR-5-340 reveals unexpected binding site, Proc. Natl. Acad. Sci. USA 116 (2019) 19109–19115.
[44] B. Yadav, K. Wennerberg, T. Aittokallio, J. Tang, Searching for drug synergy in complex dose-response landscapes using an interaction potency model, Comput. Struct. Biotechnol. J. 13 (2015) 504–513.
[45] M. Yadav, M. Igarashi, N. Yamamoto, Dynamic residue interaction network analysis of the oseltamivir binding site of N1 neuraminidase and its H274Y

mutation site conferring drug resistance in influenza A virus, PeerJ 9 (2021) e11552.
[46] Y. Zhang, A.A. Simpson, R.M. Ledford, C.M. Bator, S. Chakravarty, G.A. Skochko, T.M. Demenczuk, A. Watanyar, D.C. Pevear, M.G. Rossmann, Structural and virological studies of the stages of virus replication that are affected by antirhinovirus compounds, J. Virol. 78 (2004) 11061–11069.
[47] S. Zheng, W. Wang, J. Aldahdooh, A. Malyutina, T. Shadbahr, Z. Tanoli, A. Pessia, J. Tang, SynergyFinder Plus: toward better interpretation and annotation of drug combination screening datasets, Genom. Proteom. Bioinforma. 20 (2022) 587–596.